A new partial volume segmentation approach to extract bladder wall for computer aided detection in virtual cystoscopy

Lihong Li*[1,2], Zigang Wang[2], Xiang Li[3], Xinzhou Wei[4], Howard L. Adler[5], Wei Huang[2], Syed Rizvi[1], Hong Meng[2], Donald P. Harrington[2], and Zhengrong Liang[2]

Dept. of [1]Engineering Science and Physics, College of Staten Island, City University of New York, Staten Island, NY
Dept. of [2]Radiology and [5]Urology, State University of New York, Stony Brook, NY
Dept. of [3]Radiation Oncology, Columbia University, New York, NY
Dept. of [4]Electrical Engineering and Telecommunication, New York City College of Technology, City University of New York, Brooklyn, NY

ABSTRACT

We propose a new partial volume (PV) segmentation scheme to extract bladder wall for computer aided detection (CAD) of bladder lesions using multispectral MR images. Compared with CT images, MR images provide not only a better tissue contrast between bladder wall and bladder lumen, but also the multispectral information. As multispectral images are spatially registered over three-dimensional space, information extracted from them is more valuable than that extracted from each image individually. Furthermore, the intrinsic T_1 and T_2 contrast of the urine against the bladder wall eliminates the invasive air insufflation procedure. Because the earliest stages of bladder lesion growth tend to develop gradually and migrate slowly from the mucosa into the bladder wall, our proposed PV algorithm quantifies images as percentages of tissues inside each voxel. It preserves both morphology and texture information and provides tissue growth tendency in addition to the anatomical structure. Our CAD system utilizes a multi-scan protocol on dual (full and empty of urine) states of the bladder to extract both geometrical and texture information. Moreover, multi-scan of transverse and coronal MR images eliminates motion artifacts. Experimental results indicate that the presented scheme is feasible towards mass screening and lesion detection for virtual cystoscopy (VC).

Keywords: Virtual Endoscopy, Partial Volume Segmentation, Computer Aided Detection, MRI-based Virtual Cystoscopy, Non-invasive Screening.

1. INTRODUCTION

Bladder cancer is the fifth leading cause of cancer deaths in the United States. Over 56,500 cases of developed bladder carcinoma and more than 12,600 deaths were reported in 2002 [1]. In the last decade, the occurrence of bladder malignances has increased by 36% [2]. A common test for bladder cancer is urine dipsticks or standard urinalysis, which can be tested at home. Its sensitivity and specificity are approximately 90% and 70%, respectively [3]. However, the finding is usually at the very late stage and unable to provide the accurate location and size of the lesion.

While currently available cystoscopy is the most accurate diagnostic procedure for detecting the lesion, it is invasive, expensive, uncomfortable, lacks an objective scale and has limited field-of-view (FOV). It isn't indicative or applicable in patients with severe urethral strictures or active vesical bleeding. Patients are usually reluctant for such examination. Therefore, a minimal or non-invasive, safe, and low-cost method to evaluate the bladder would be preferred by most patients.

Recently, virtual cystoscopy (VC) has been developed as an alternative means for early diagnosis of bladder abnormalities. Several clinical VC feasibility studies have been reported [4-7], based on computer tomography (CT) technologies. Because the earliest stages of bladder lesion development are inside the mucosa with gradual extension

*Correspondence: li@postbox.csi.cuny.edu; phone 718 982-2993; fax 718 982-2830; Image Processing and Computer Vision Research Laboratory, Department of Engineering Science and Physics, College of Staten Island, City University of New York, Staten Island, NY 10314.

Medical Imaging 2004: Physiology, Function, and Structure from Medical Images, edited by Amir A. Amini, Armando Manduca, Proceedings of SPIE Vol. 5369 (SPIE, Bellingham, WA, 2004) · 1605-7422/04/$15 · doi: 10.1117/12.535913

into bladder muscle, a desirable "visual gradient" between bladder lumen and wall is required for differentiating the associated structures [8, 9]. However, in CT images, bladder muscle has no contrast difference from the lumen filled with urine. Although bladder insufflation with room air or CO_2 via a Foley catheter is feasible to obtain the contrast between bladder wall and the lumen, it is invasive and unable to acquire the contrast among the tissues in the wall/mucosa. Therefore, CT-based VC can only detect the lesions with significantly-developed geometry information. The lack of tissue contrast, as well as the uncomfortable invasive insufflation procedure (which may induce infection), become the major limitation of its ability for early detection of bladder lesions.

By magnetic resonance (MR) imaging technologies, VC has shown its potential in early investigation of bladder lesion [10, 11, 12]. MR images provide not only a better tissue contrast from bladder wall to the lumen (without air insufflation), but also the multi-spectral information, as compared to the CT images. As multi-spectral (T_1- and T_2-weighted) MR images are spatially registered over three-dimensional (3D) space, information extracted by means of image processing from images is obviously more valuable than that extracted from each image individually. Furthermore, the intrinsic T_1 and T_2 contrast of the urine against the bladder wall eliminates completely the invasive air insufflation procedure. Because the earliest stages of bladder lesion development are in the mucosa with gradual extension into bladder muscle, in this paper, we focus our attention on the mucosa layer of the bladder wall for computer aided detection of the bladder lesions.

2. METHODS

It is expected that early sign of bladder lesion would be reflected by both the morphology and texture on the bladder wall and mucosa. The morphological difference and texture variation could appear on the bladder wall when the bladder lumen is in different states, e.g., full of urine or near empty. To suppress motion artifacts, multi-scan of transverse and coronal multispectral MR images were acquired at empty and full states, respectively. Our mixture-based scheme specifies on quantifying images as percentages of tissues inside that voxel. This mixture-based image segmentation has unlimited spatial resolution on the tissue boundaries and provide tissue growth tendency in addition to the anatomical structure of the tissue. We further developed a computer aided diagnosis and detection system based on the mixture segmentation. Experimental studies on patients are promising. In this paper, we proposed a novel mixture-based computer aided diagnosis system using multispectral MR images.

2.1 MRI data acquisition

Multispectral MR images were acquired by a Phillips 1.5 T Edge whole-body scanner with the body coil as the transceiver. A spoiled-GRASS sequence was employed to acquire T_1-weighted transverse images with parameter of 256x256 matrix size, 38 cm FOV, 1.5 mm slice thickness, T_E=3 ms, T_R=9 ms, 30 degree flip angle, and one-scan average. With the same acquisition parameters, a T_1-weighted coronal image was acquired. Correspondingly, an axial FSE sequence was used to collect T_2-weighted transverse images with the same acquisition location and parameters, except for T_E=96 ms, T_R=12167 ms, 90 degree flip angle, and two-scan average. Then, a coronal FSE sequence was used for acquiring the T_2-weighted coronal images.

Dual states of MR imaging were designed for the study. After the patient voided, patient was asked to drink a cup of water. Images of the nearly empty state of the bladder were acquired first. Waiting for a while, when the patient feels bladder full, full state images were acquired. The dual states of multi-scan scheme provide both geometric and texture information.

In T_1-weighted images, there exists an observable contrast between urine lumen and bladder wall as well as between bladder wall and other surrounding tissues (Fig. 1a). The bladder wall thickness becomes thicker in the empty states (Fig. 1b). However, the boundary between bladder wall and rectum wall becomes very vague. On the other hand, T_2-weighted images provide reciprocal information with a brighten urine lumen to be distinguished easily from other tissues (Fig. 1c and Fig. 1d).

The image acquisition time is about 2 to 5 minutes for obtaining a T_1-weighted image. During this period, it is unlikely for patients to hold a single breath. Therefore, motion artifacts are expected along the direction of spine in the transverse

images. In order to overcome this artifact, a corresponding coronal image is obtained in the meantime. It is expected that this multi-scan scheme will reduce false positive (FP) in lesion detection.

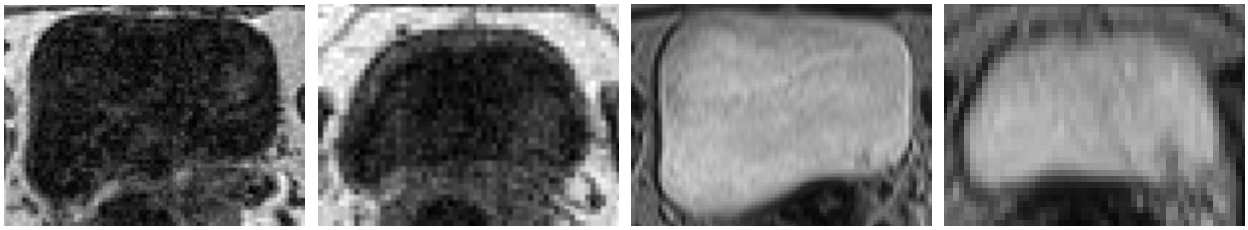

(a) (b) (c) (d)

Fig 1. (a) One slice of a T_1-weighted image at the full state. (b) One slice of a T_1-weighted image at the empty state, where the thickness of the bladder wall is thicker than that at the full state. (c) One slice of a T_2-weighed image at the full state, where the urine lumen could be easily distinguished. (d) One slice of a T_2-weighed image at the empty state.

2.2 Image processing

A 3D interpolation procedure was first applied to the datasets to construct isotropic voxels in the 3D domain. The size of dataset was expanded from 256x256xn to 512x512xm, where n was the slice number of the original dataset and m was the slice number of the interpolated dataset [13, 14]. Following that, a new PV segmentation algorithm was developed to achieve mixture segmentation and extract the bladder wall.

Given the l element of multispectral images $Y = \{Y_{il}\}$, $i = 1, 2, \ldots, I$, over the total number of voxels in the acquired image, let M be a set of vectors $M = \{m_1, \ldots, m_2, \ldots, m_I\}$, where m_{ik} reflects the fraction of tissue type k inside voxel i. Each y_{il} follows a random process as

$$y_{il} = \sum_{k=1}^{K} m_{ik}\mu_{kl} + n_{il} \tag{1}$$

where μ_{kl} denotes the mean of class k; m_{ik} is the probability of voxel i belonging to class k; and n_{il} is the Gaussian noise with zero mean and variance of σ_{il}. An Expectation and Maximization (EM) algorithm was utilized to achieve robust model parameter estimation [15, 16] as

$$\mu_{kl}^{(n+1)} = \frac{\sum_i x_{ikl}^{(n)}}{\sum_i m_{ik}} \tag{2}$$

$$\sigma_{kl}^{(n+1)} = \frac{1}{N}\sum_i \frac{(x_{ikl}^2)^{(n)} - 2m_{ik}\mu_{kl}^{(n+1)}x_{ikl}^{(n)} + (m_{ik}\mu_{kl}^{(n+1)})^2}{m_{ik}} \tag{3}$$

where x_{ikl} is the contribution of tissue type k to the observation of y_{il} and

$$x_{ikl}^{(n)} = m_{ik}\mu_{kl}^{(n)} + \frac{m_{ik}\sigma_{kl}^{n}}{\sum_{j=1}^{k} m_{ij}\sigma_{jl}^{(n)}} \cdot (y_{il} - \sum_{j=1}^{K} m_{ij}\mu_{jl}^{(n)}) \ . \tag{4}$$

The PV segmentation is performed by a maximum *a posterior* (MAP) principle, where a Markov random field (MRF) model-based prior [17-20] is applied.

After image segmentation, a mixture (mucosa) layer indicating the bladder wall was obtained directly from the algorithm. By choosing a seed point from the lumen, the bladder lumen could be extracted by means of region growing

algorithm. Fig. 2 shows a slice of T_1- and T_2- weighted transverse images, and the corresponding extracted mucosa layer.

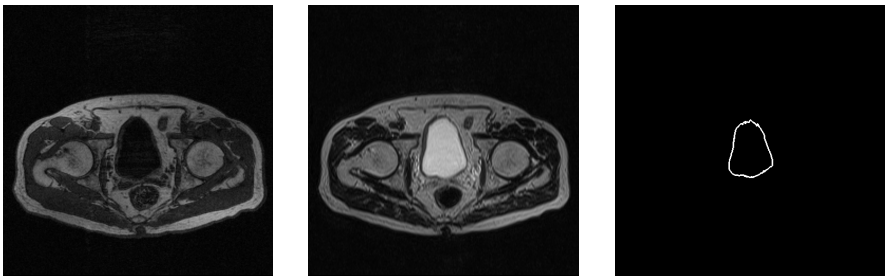

(a) (b) (c)

Fig. 2. (a)-(b): A slice of T_1-weighted and T_2-weighted images in the transverse scan. (c) The extracted mucosa layer indicating bladder lumen wall.

2.3 Display system

Registration is needed for simultaneously displaying the dual states of bladder. In practice, physician will perform an initial inspection before examining the abnormal section. Therefore, a perfect registration isn't necessary. In this study, we calculated the central mass of the bladder and chose the central mass as a reference for registration.

Dual states of bladder (full and near empty) and multi-scans (transverse and coronal) are viewed simultaneously through different windows. At each state, we reconstruct both inner and outer bladder wall from the mixture-based segmentation [21]. Furthermore, the system provides physicians with two-view direction (from outside and inside). Physicians can view bladder at any angle and any distance. When the physician rotates the bladder in one window, the system will calculate the relative parameter, and rotate the bladder at the other three windows to display the same section of the bladder. In addition, a transparent attribute is designed for physicians to view the whole bladder transparently.

2.4 Computer aided detection

To detect the abnormal section from the bladder datasets, we developed a mixture based detection method [22]. A 3D geometrical feature extraction algorithm is applied to extract the principal curvature, shape index, and curvedness of each mixel. The extracted geometry information is utilized to distinguish bladder lesions from the normal bladder wall.

2.4.1 Extracting 3D geometrical feature

For each tissue element, there exists an iso-intensity surface across through that element volume. Principal direction and curvature are two important geometrical attributes of the 3D surface. To describe the shape of the surface, Dorai [23] presented two quantitative measures for a given point p: Shape Index SI and Curvedness R. They are defined as:

$$SI(p) = \frac{1}{2} - \arctan\frac{k_1(p) + k_2(p)}{k_1(p) - k_2(p)} \tag{5}$$

$$R(p) = \sqrt{\frac{k_1(p)^2 + k_2(p)^2}{2}} \tag{6}$$

where $k_1(p)$ and $k_2(p)$ are the principal curvatures, and $k_1(p) \geqslant k_2(p)$. It is noted that the SI represents what kind of type the surface is, while the R represents what "curve" this surface is.

Given a mixel m_{ik}, there are several tissue elements in that mixel. We extract its principal curvature, shape index and curvedness and describe the shape information of this mixel. However, the shape information only reflects a relative "local shape" relation between this mixel and its corresponding neighborhood. On the other hand, the "global shape"

information provides an approximate shape description for a larger region, therefore describing the whole shape field. By applying the linear integral convolution (LIC) algorithm [24], we built two principal directions to construct a dual vector volume, i.e., two convoluted curvatures are obtained after the LIC. These two curvatures reflect the "global" shape of the object. We can utilize Eq. (5) and Eq. (6) to compute two new terms, $SI^g(p)$ and $R^g(p)$, i.e., "global shape index" and "global curvedness". Similar to the local shape index and curvedness, global shape information also provides a quantitative measure of the object shape.

2.4.2 Detection of bladder lesions

Normal bladder wall usually has regular shapes that are described as "elliptic curvature." That is, the shape description of the inner bladder wall should be "spherical cup" or "trough." This shape description can be applied to distinguish the bladder lesion from the normal bladder wall. For those irregular sections in the bladder wall without smooth surface, the variance the local shape index value of the bladder wall may not as smooth as that of the regular wall. If only based on the "local" geometrical shape information, FP detections will be easily produced. We evaluated the corresponding "global" shape index and found its variance remains smooth for most of the irregular bladder wall section. Therefore, all mixels whose "global" shape description is different from that of the normal bladder wall are extracted first. Based on the connectivity in the 3D space, all selected mixels are clustered into several groups, which are called as initial bladder lesion candidates.

The initial bladder lesion candidates can be further divided into three groups: real bladder lesions, noise candidates, and mimic candidates. Noise candidates are usually generated due to MR imaging scan, patient movement, or segmentation error, which induces several little protuberance regions on the bladder wall. According to our observation, they are usually very small with a tiny spherical top section. On the other hand, the mimic candidates are generated due to normal tissues such as bladder tube and small tissue pieces connected to the bladder wall. Both noise and mimic candidates are called FP candidates. In order to eliminate FP candidates, we utilized the following filtering steps in our method.

1) If the total voxel number of the candidate is small, this candidate will be classified as a FP candidate. Similarly, if the size of the continuous spherical top in either local or global geometrical measure is small, this candidate will be classified as a FP candidate.
2) If the position of the initial lesion candidate whose "local" and "global" general shapes do not lie in the spherical shape domain, this candidate is a FP candidate.

3. RESULTS

Two patients and four healthy male volunteers were recruited in this study. An interactive display system has been developed for viewing inner and outer bladder walls. Fig. 3 shows the outer view of transverse and coronal scans of bladder at two states, full and near empty. While Fig. 4 shows the inner view of transverse and coronal scans of bladder at two states. The interactive system allows physicians to view bladder at any angle and any distance. Physicians can also rotate the bladder and zoom in to inspect the abnormalities. The advantages of multi-scans have shown in Fig. 5, where small artifacts appeared in the transverse scans but disappeared in the coronal scans. The presented multi-scan scheme provides us complementary information, therefore increasing the detection accuracy.

Perfect detection results were obtained from volunteer studies, as expected. In the patient study as shown in Fig. 6, one lesion with a size of 25-30 mm was detected at both states. A small one with 8-10 mm size was detected in the full state while missed in the empty state. When the scheme examined the texture information at the corresponding location in the empty state, this small one becomes a candidate. All candidates were finally examined by the physician using the display system.

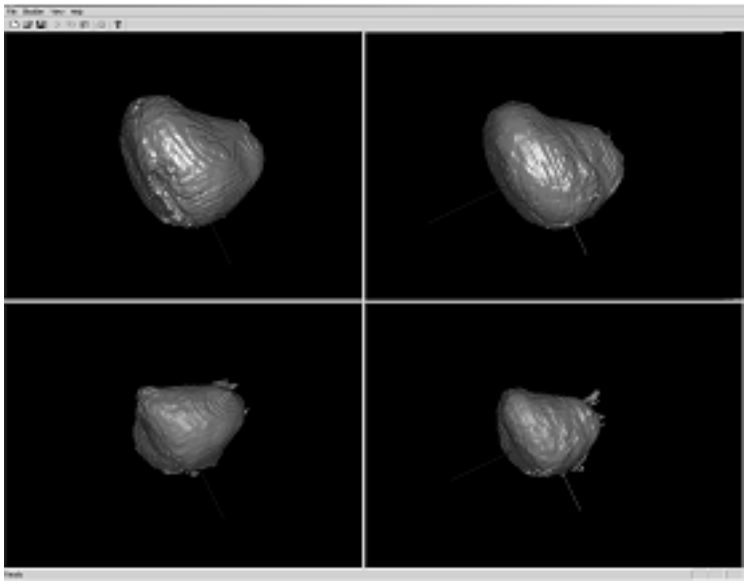

Fig. 3. The outer view of transverse (left) and coronal (right) scans of bladder at two states, full (top) and near empty (bottom).

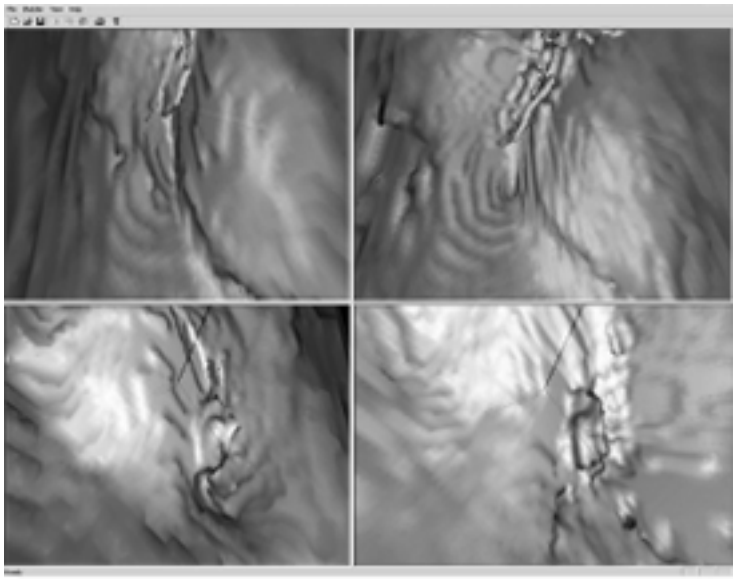

Fig. 4. The inner view of transverse (left) and coronal (right) scans of bladder at two states, full (top) and near empty (bottom).

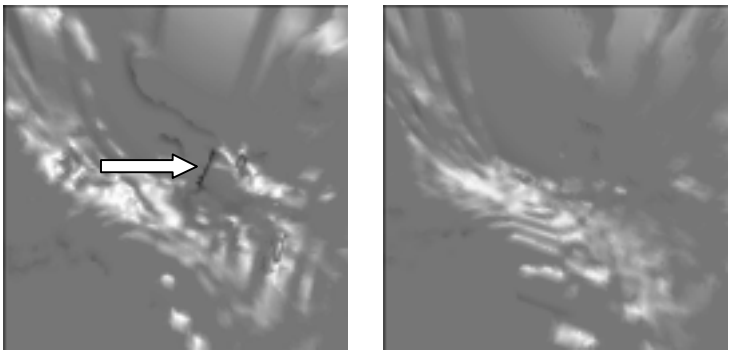

Fig. 5. Small artifacts appear in the transverse scan (left), while the corresponding coronal scan (right) provides a smooth view.

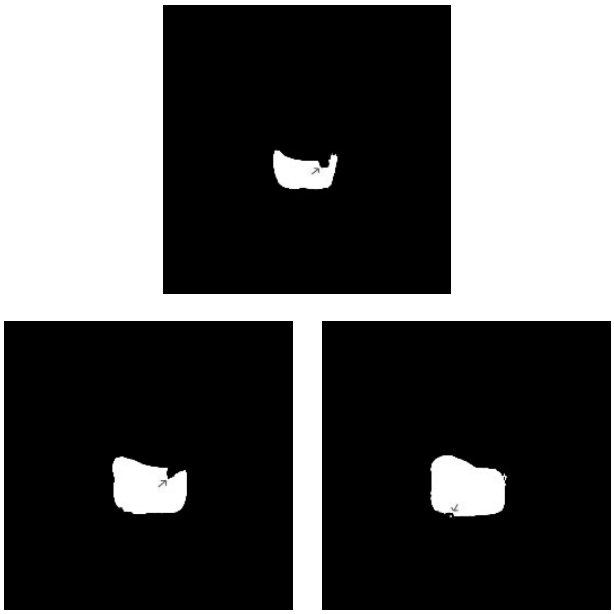

Fig. 6. One lesion with size of 25-30 mm was detected at both empty state (top) and full state (bottom left). A small one with size of 8-10 mm was detected in the full state (bottom right).

4. DISCUSSIONS AND CONCLUSIONS

We have developed a new PV segmentation scheme to extract the bladder wall for CAD of bladder lesions using multispectral MR images. The presented scheme is a non-invasive, user-friendly, and patient-comfortable procedure. From the experiment results, we conclude that information extracted from multispectral MR images provides us much more valuable information than that from each image individually. The dual states of bladder provide dynamic (both geometric and texture) information. In addition, multi-scan images overcome breathing motion artifacts. Experimental results indicate the present scheme is feasible towards mass screening and lesion detection. Further evaluations on a large number of patient datasets are under progress.

ACKNOWLEDGMENT

This work was supported in part by the National Institutes of Health under Grant No. CA82402 and the Research Foundation of the City University of New York. The volunteer and patient datasets were acquired at the University Hospital of the State University of New York at Stony Brook.

REFERENCES

1. A. Jemal, A. Thomas, T. Murray, and M. Thun, "Cancer statistics," *CA Cancer J. Clin.*, vol. 52, pp. 23-47, 2002.
2. D. L. Lamm and F. M. Torti, "Bladder cancer," *CA Cancer J. Clin.*, vol. 46, pp. 93-112, 1996.
3. S. T. Shaw, S. Y. Poon, and E. T. Wong, "Routine urinalysis: Is the dipstick enough?" *JAMA*, vol. 253, pp. 1596-1600, 1985.
4. H. M. Fenlon, T. V. Bell, H. K. Ahari, and S. Hussain, "Virtual cystoscopy: Early clinical experience," *Radiology*, vol. 205, No. 1, pp. 272-275, 1997.
5. S. Hussain, J. A. Loeffler, R. K. Babayan, and H. M. Fenlon, "Thin-section helical computer tomography of the bladder: Initial clinical experience with virtual reality imaging," *Urology*, vol. 50, No. 5, pp. 685-689, 1997.
6. M. Merkle, A. Wunderlich, A. J. Aschoff, N. Rilinger, J. Gorich, R. Bachor, H. W. Gottfried, R. Sokiranski, T. R. Fleiter, and H. J. Brambs, "Virtual cystoscopy based on helical CT scan datasets: Perspectives and limitations," *The British Journal of Radiology*, vol. 71, pp. 262-267, 1998.
7. D. J. Vining, R. J. Zagoria, K. Liu, and D. Stelts, "CT cystoscopy: An innovation in bladder imaging," *AJR*, vol. 166, pp. 409-410, 1996.
8. G. Prout, "Bladder cancinoma," *Surgical Oncology*, pp. 679-697, McGraw Inc., New York, 1984.
9. J. R. Fielding, L. Hoyte, S. A. Okon, A. Schreyer, J. Lee, K. H. Zou, S. Warfield, J. P. Richie, K. R. Loughlin, M. P. O'leary, C. J. Doyle, and R. Kikinis, "Tumor detection by virtual cystoscopy with color mapping of bladder wall thickness," *Journal of Urology*, vol. 167, pp. 559-562, 2002.
10. Z. Liang, D. Chen, T. Button, H. Li, and W. Huang, "Feasibility studies on extracting bladder wall from MR images for virtual cystoscopy," *Proc. Intl. Soc. Mag. Reson. Med.*, pp. 2204, 1999.
11. D. Chen, B. Li, W. Huang, and Z. Liang, "A multi-scan MRI-based virtual cystoscopy," *SPIE Medical Imaging*, vol. 3978, pp. 146-152, 2000.
12. L. Li, Z. Wang, D. Harrington, W. Huang, and Z. Liang, "A Mixture-based Computed Aided Detection System for Virtual Cystoscopy," *Proc. Intl. Soc. Mag. Reson. Med*., pp.1466, 2003
13. L. Li, X. Li, W. Huang, C. Christodoulou, D. Chen, A. Tudorica, P. Djuric, L. Krupp, and Z. Liang, "A novel mixture-based segmentation algorithm for quantitative analysis of multiple sclerosis using multispectral MR images," *Proc. Intl. Soc. Mag. Reson. Med.*, pp. 354, 2002.
14. L. Li, X. Li, H. Lu, W. Huang, C. Christodoulou, A. Tudorica, L. B. Krupp, and Z. Liang, "MRI volumetric analysis of Multiple Sclerosis: Methodology and validation," *IEEE Trans. Nuclear Science*, vol. 50, pp. 1686-1692, 2003.
15. X. Li, D. Eremina, L. Li, and Z. Liang, "Partial volume segmentation of medical images," *IEEE Medical Imaging Conference Record*, 2003.
16. Z. Liang, X. Li, D. Eremina, and L. Li, "An EM framework for segmentation of tissue mixtures from medical images", *Intl Conf of IEEE Engineering in Medicine and Biology*, Concun, Mexico, pp. 682-685, 2003
17. R. Leahy, T. Hebert, and R. Lee, "Applications of Markov random fields in medical imaging," *Information Processing in Medical Imaging*, pp. 1-14, 1991.
18. Z. Liang, R. J. Jaszczak, and R. E. Coleman, "Parameter estimation of finite mixtures using the EM algorithm and information criteria with application to medical image processing," *IEEE Trans. Nuclear Science*, vol. 39, pp. 1126-1133, 1992.
19. Z. Liang, J. R. MacFall, and D. P. Harrington, "Parameter estimation and tissue segmentation from multispectral MR images," *IEEE Trans. Medical Imaging*, vol. 13, pp. 441-449, 1994.
20. K. Held, E. R. Kops, B. J. Krause, W. M. Wells, R. Kikinis, and H. Muller-Gartner, "Markov random field segmentation of brain MR images," *IEEE Trans. Medical Imaging*, vol. 16, pp. 876-886, 1997.
21. Z. Wang and Z. Liang, "Feature based rendering for 2D/3D partial volume segmentation datasets," *SPIE Medical Imaging*, vol. 4681, pp. 681-687, 2002.
22. Z. Wang, L. Li, X. Li, Z. Liang, and D. P. Harrington, "Skeleton based 3D computer aided detection of colonic polyps," *SPIE Medical Imaging*, vol. 5032, pp. 843-853, 2003.
23. C. Dorai and A. K. Jain, "COSMOS - A Representation scheme for 3D free-form objects", *IEEE Trans. Pattern Analysis and Machine Intelligence*, vol. 45, pp. 2132-2138, 1997.
24. B. Cabral and L. Leedom, "Imaging vector fields using line integral convolution", *ACM SIGGRAPH Computer Graphics, Proceedings of the 20th Annual Conference on Computer Graphics*, pp. 263-270, 1993.